

Received May 5, 2020, accepted May 30, 2020, date of publication June 5, 2020, date of current version June 17, 2020.

Digital Object Identifier 10.1109/ACCESS.2020.3000289

Label-Free Identification of Early Gastrointestinal Neuroendocrine Tumors via Biomedical Multiphoton Microscopy and Automatic Image Analysis

LIANHUANG LI¹, SHENGHUI HUANG², LIDA QIU^{1,3}, WEIZHONG JIANG², ZHIFEN CHEN², DEYONG KANG⁴, HAOHUA TU⁵, JIANXIN CHEN¹, AND YONGJIAN ZHOU⁶

¹Key Laboratory of Optoelectronic Science and Technology for Medicine of Ministry of Education, Fujian Provincial Key Laboratory of Photonics Technology, Fujian Normal University, Fuzhou 350007, China

²Department of Colorectal Surgery, Fujian Medical University Union Hospital, Fuzhou 350001, China

³College of Physics and Electronic Information Engineering, Minjiang University, Fuzhou 350108, China

⁴Department of Pathology, Fujian Medical University Union Hospital, Fuzhou 350001, China

⁵Beckman Institute for Advanced Science and Technology, University of Illinois at Urbana-Champaign, Urbana, IL 61801, USA

⁶Department of Gastric Surgery, Fujian Medical University Union Hospital, Fuzhou 350001, China

Corresponding authors: Lianhuang Li (lhli@fjnu.edu.cn) and Yongjian Zhou (zhouybju@163.com)

This work was supported in part by the National Natural Science Foundation of China under Grant 81671730, Grant 61972187, and Grant 81602798, in part by the Natural Science Foundation of Fujian Province under Grant 2019J01269, Grant 2019J01761, Grant 2018J01301, and Grant 2018J01183, in part by the Joint Funds for the Innovation of Science and Technology of Fujian Province under Grant 2017Y9038, in part by the Program for Changjiang Scholars and Innovative Research Team in University under Grant IRT_15R10, and in part by the National Institutes of Health under Grant R01 CA241618.

ABSTRACT At present, early diagnosis and treatment is the most effective way to treat early gastrointestinal neuroendocrine tumors. Therefore, we attempted to carry out multiphoton imaging of early neuroendocrine tumors because of its ability to label-free image tissue microstructure at the cellular level. Imaging results show that this imaging technique can quickly identify the histopathological changes in mucosa and submucosa caused by tumor invasion. Furthermore, we performed automatic image analysis on SHG images and extracted two optical diagnostic features—collagen density and average intensity, and also found obvious differences in the density as well as average intensity of collagen fibers in tumor microenvironment using a series of quantitative analysis. These findings may further facilitate the development of multiphoton microscopic imaging technique for clinical use.

INDEX TERMS Multiphoton imaging, image analysis, gastrointestinal neuroendocrine tumors.

I. INTRODUCTION

In recent several years, gastrointestinal neuroendocrine neoplasms get more and more attention because they are on the rise likely as a result of more endoscopy being done [1]–[3]. They are often indolent and generally slow growing tumors, but can also be very aggressive and metastasize widely [4], [5]. These tumors may be diagnosed accidentally, or as part of the work-up for upper gastrointestinal bleeding, anemia, or non-specific abdominal pain [6], and thus their diagnosis is often delayed. Early neuroendocrine tumors which do not invade into muscularis propria were reported to have a good prognosis because they generally

have a low risk of distant metastasis and spread [7]. Previous study showed that tumor invasion depth was one of the most powerful prognostic factors affecting clinical outcome in patients [8], [9]. For patients with gastrointestinal neuroendocrine tumors, the overall five-year survival rate has gone up by nearly 20% in the past 35 years largely due to early detection [10], [11]. At present, endoscopic screening is an effective means in the early diagnosis of neuroendocrine tumors; however, its diagnostic accuracy still needs to be improved. As a consequence, it is necessary and meaningful to develop an effective tool for accurately identifying early neuroendocrine neoplasms.

Multiphoton microscopy (MPM) is an emerging nonlinear optical imaging technology which can generate cellular resolution images from unprocessed or unstained tissues [12].

The associate editor coordinating the review of this manuscript and approving it for publication was Chao Zuo¹⁰.

According to previous publications, there were many components in biological tissues that would produce endogenous optical signals, for example, nicotinamide adenine dinucleotide (NAD) and flavin adenine dinucleotide (FAD) in cells can emit two-photon autofluorescence (TPAF) signal and extracellular collagen matrix can generate second-harmonic generation (SHG) signal [13], [14]. Therefore, MPM which is mainly grounded on the TPAF as well as SHG imaging has been shown to be able to afford histology-like images of biological tissues, and has been widely used in imaging research of various tissues: Mehidine et al used multimodal multiphoton imaging to study human normal brain tissues as well as brain tumor tissues [15], Li et al revealed quantitative difference in the premalignant and malignant stomach mucosa by endogenous multiphoton signals [16], and Sun et al used second-harmonic generation microscopy to image and quantify liver fibrosis ex vivo [17], and so on. In the present study, we introduced this novel optical diagnostic tool—MPM (including TPAF and SHG imaging) to detect early neuroendocrine neoplasms in gastrointestinal tract and thereby evaluated the feasibility of using this technique to diagnose these tumors.

II. MATERIALS AND METHODS

A. SAMPLE PREPARATION

This research work was performed after the approval of the institutional review board at the Fujian Medical University Union Hospital, and before study, every patient signed an informed consent. Five fresh samples from 5 patients were collected, and normal tissues were also collected for comparative analysis. Once tissues were surgically removed, they were taken to the pathology department immediately for frozen sections. A slice ($10\ \mu\text{m}$ thickness) was used for label-free optical imaging, and for confirmation, a neighbor slide was stained with the hematoxylin and eosin (H&E). A digital image of each H&E-stained section firstly checked by pathologist was taken via an optical microscope (Eclipse Ci-L, Nikon Instruments Inc., Japan) with a CCD (DS-Fi2, Nikon). In our experiment, we first dripped small amounts of phosphate-buffered saline (PBS) on the fresh tissue slice for the purpose of preventing dehydration or shrinkage, and then a cover slip was put on the section for multiphoton imaging.

B. BIOMEDICAL MULTIPHOTON MICROSCOPY

This imaging equipment has been explained in detail in our previous work [18]. All the multiphoton images were captured via an microscope (LSM 510, Zeiss, Germany) which was inverted and equipped with a femtosecond Ti:sapphire laser (Mira 900-F, Coherent, Inc., USA). A Zeiss Plan Apochromat oil-immersion objective lens ($63\times$, NA=1.4) was applied to acquire high-resolution images, and the laser power at the focal plane of the objective is about 10mW. In this study, TPAF signal (a wavelength range of 430–716 nm) and SHG signal (a wavelength range from 389 to 419 nm) were collected respectively by a META detector

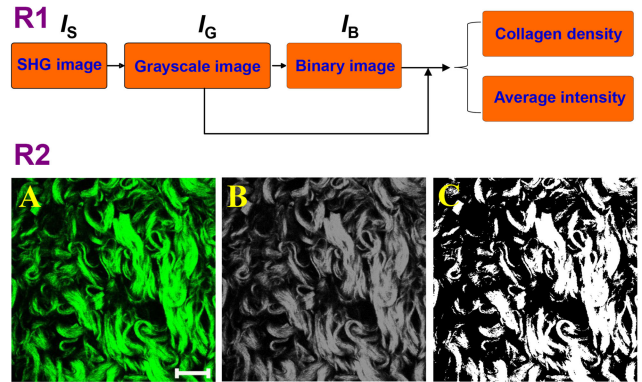


FIGURE 1. Row 1: a flowchart of automatic image processing strategy for quantifying collagen density and average intensity from the SHG images; Row 2: a schematic of quantitative analysis: (A) Original SHG image (512×512 pixels); (B) Grayscale image; (C) Binary image using threshold based on the Otsu's method. Scale bar: $20\ \mu\text{m}$.

using $810\ \text{nm}$ wavelength laser. For this imaging system, a lateral resolution of $0.3\ \mu\text{m}$ could be achieved, and it takes $1.8\ \mu\text{s}$ for collecting each pixel and therefore the scanning speed is 2 frames per second (512×512 pixels/ $135\ \mu\text{m} \times 135\ \mu\text{m}$). We can acquire large-area MPM image through automatically assembling an array of images with 512×512 pixels via ZEN imaging software.

C. QUANTITATIVE ANALYSIS

To obtain some quantitative optical diagnostic features, we used automated image processing strategy to analysis the SHG images of each slide, and two parameters—SHG average intensity and collagen density—were extracted. For each SHG image, the average intensity is computed through dividing the total of SHG intensities by all SHG pixels, and collagen density is defined as a ratio of SHG pixels to all image pixels. A flowchart of image processing was shown in Figure 1: every SHG image (I_S) was first converted to a grayscale image (I_G), and then a binary image (I_B) derived from the associated grayscale image was created with a threshold generated by the Otsu's method [19], in which the pixel was replaced with a value 1 (white) if its luminance was greater than the threshold and meanwhile another pixels were replaced with a value 0 (black), here these pixels with value 1 indicated the collagen distribution region; finally, the grayscale images and binary images were used together to compute the collagen density and average intensity.

For a given SHG image with $N \times M$ pixels, the collagen density and average intensity can be obtained based on the following formulas:

$$\text{Collagen density} = \frac{1}{NM} \sum_{n=1}^N \sum_{m=1}^M I_B(n, m) \quad (1)$$

$$\text{Average intensity} = \frac{1}{NM} \sum_{n=1}^N \sum_{m=1}^M I_G(n, m) \quad (2)$$

where $I_B(n, m)$ denotes the binary value at the pixel location (n, m) of binary image, and $I_G(n, m)$ indicates the intensity

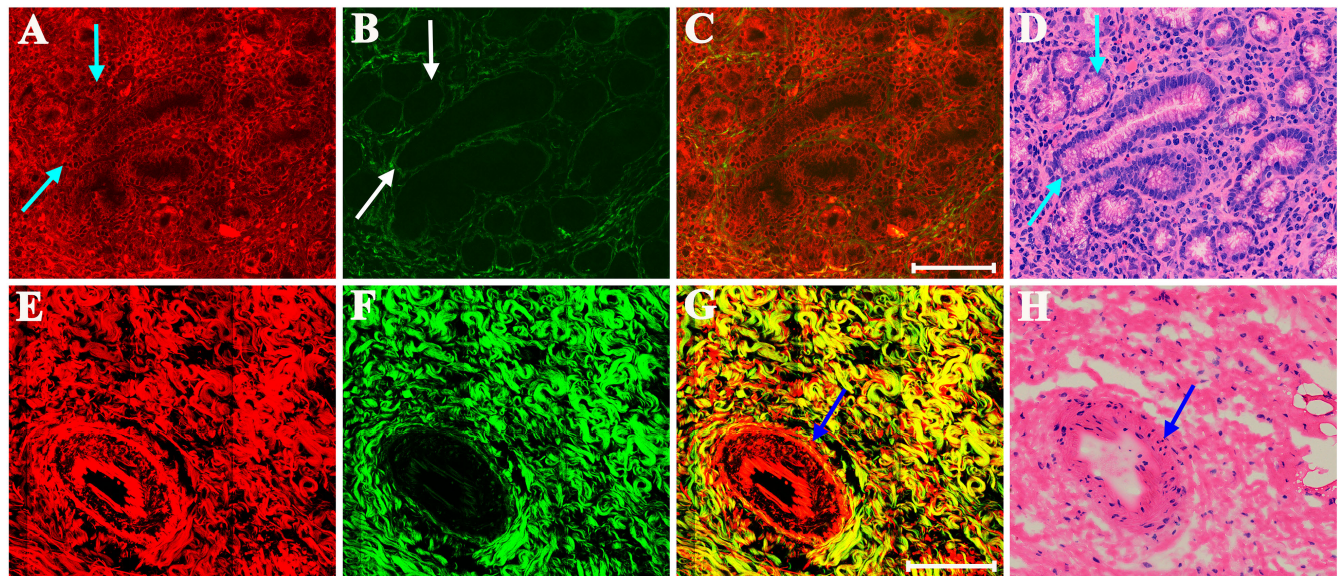


FIGURE 2. Row1: MPM images of normal mucosa and a corresponding H&E-stained image, (A) TPAF image, (B) SHG image, (C) Composite image, (D) H&E-stained image ($40\times$); Row2: MPM images of normal submucosa and a corresponding H&E-stained image, (E) TPAF image, (F) SHG image, (G) Composite image, (H) H&E-stained image ($40\times$). Pseudo-color presentation in the MPM image: red—TPAF; green—SHG. Cyan arrow: normal gastric glands; white arrow: basement membrane; blue arrow: blood vessel. Scale bar: $100\mu\text{m}$.

at the pixel location (n, m) of grayscale image. Moreover, for the mucosal and submucosal layers on every slide, five randomly different images (512×512 pixels) from each layer were selected for the automated image analysis.

D. STATISTICAL ANALYSIS

The MATLAB 2018b was used for performing automatic image analysis, and R version 3.6.1 was used for all the statistical analyses. The student's t-test was chosen to evaluate statistical difference. Statistical results were displayed by an average value following a standard deviation (SD), and were thought to be difference if $P \leq 0.05$.

III. RESULTS

A. HISTOPATHOLOGIC FEATURES OF EARLY GASTROINTESTINAL NEUROENDOCRINE NEOPLASMS

Gastrointestinal neuroendocrine neoplasms demonstrate a low frequency of distant and lymph node metastasis when these primary tumors are confined within the mucosal or submucosal layer [20], and as a result are suitable for less invasive therapies. Endoscopic therapies, for instance, endoscopic mucosa resection (EMR) or endoscopic submucosal dissection (ESD), are increasingly likely to serve as the first-line treatment for these early diseases [21], [22], because they are less invasive than surgical resection and can provide improved quality of life for patients. Hence, we must precisely assess tumor invasion which has important influence on survival evaluation as well as clinical intervention. In view of this situation, we conducted a study on the identification of various pathological changes caused by early gastrointestinal neuroendocrine neoplasms based on multiphoton imaging technique.

Firstly, we used MPM to image the normal mucosal and submucosal layers of stomach for comparative analysis. As shown in Figure 2, many normal gastric glands (cyan arrow in Figure 2A) are clearly displayed via TPAF imaging, and using SHG imaging, it is easy to identify the basement membranes (white arrow in Figure 2B) which are primarily used to prop up these glands. MPM imaging also demonstrates that normal submucosa contains a large number of collagen fibers, and surprisingly, a blood vessel is detected too (blue arrow in Figure 2G). Therefore, without the need of fluorescent labeling, MPM is capable to uncover the cellular structure and morphology, and tissue microenvironment based on the endogenous TPAF and SHG signals. All these imaging results are confirmed by the digital images taken from the corresponding H&E-stained sections (Figures 2D and 2H).

Secondly, our target is the abnormal mucosa, and MPM images indicate: some glands (white arrow in Figure 3A) are still found and mucous cells with mucocyst (blue arrow in Figure 3A) could be recognized. We also find some elastic fibers (cyan arrow in Figure 3A) that are clumped together, and interestingly, these fibers only produce TPAF signal. On the other hand, SHG imaging could offer complementary information about the distinctive microstructure of biological tissues as displayed in Figure 3B, revealing different patterns of collagen distributions, for example, some collagen fibers surround the glands, while others form a network to support various cells.

Above all, some nests of neuroendocrine tumor cells (cyan dashed square in Figure 3C) are detected in lamina propria. In the zoom-in image (Figure 3E), we can see that tumor cells have formed many cancerous nests (yellow arrow

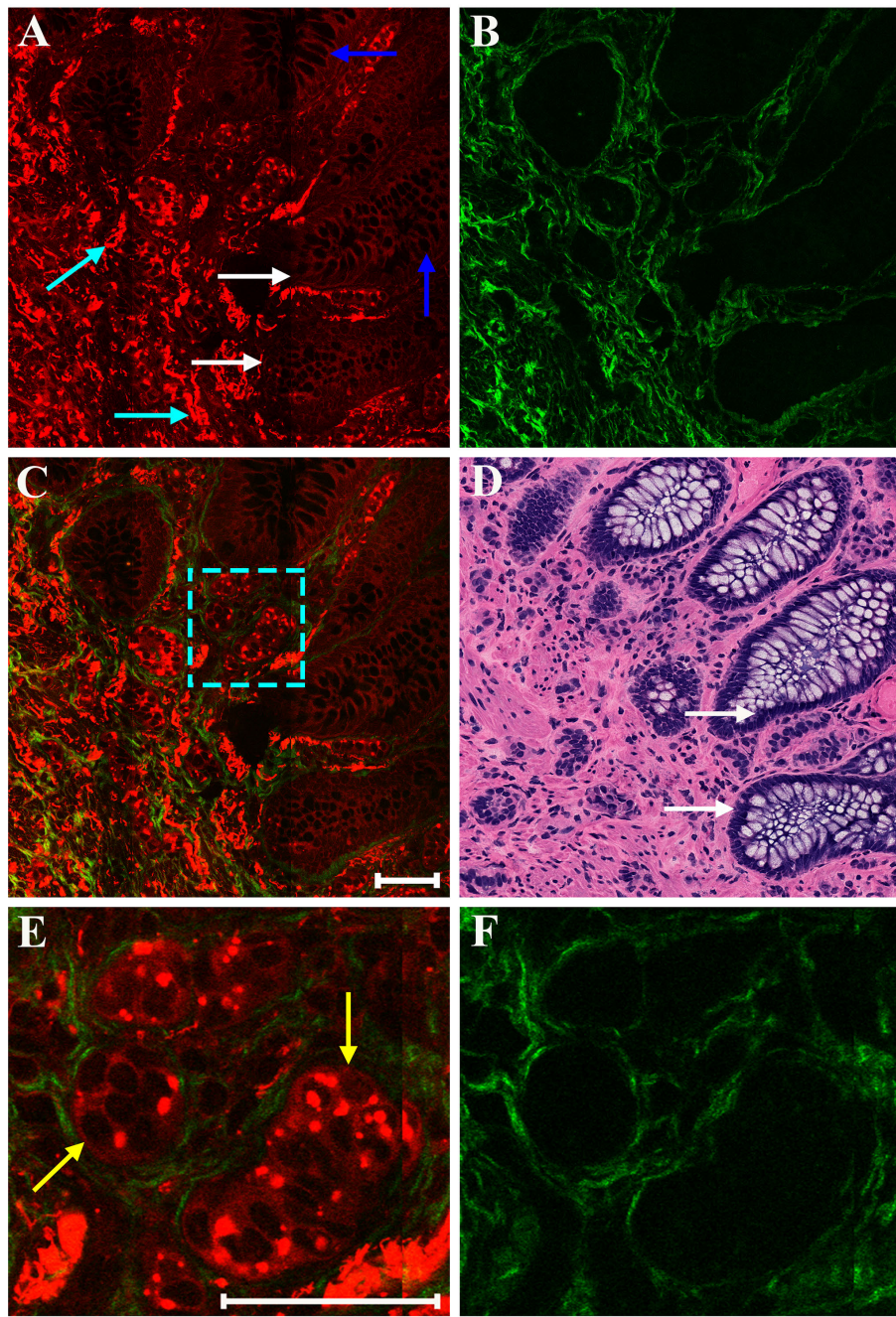


FIGURE 3. MPM images of neuroendocrine tumors invading into mucosa and a corresponding H&E-stained image: (A) TPAF image; (B) SHG image; (C) Composite image; (D) H&E-stained image ($40\times$); and (E-F) Magnified MPM and SHG images of the region of interest (cyan dashed square) respectively. Pseudo-color presentation in the MPM image: red—TPAF; green—SHG. White arrow: gastric glands; blue arrow: mucous cells; cyan arrow: elastic fibers; yellow arrow: nests of neuroendocrine tumor cells. Scale bar: $50\mu\text{m}$.

in Figure 3E), and the individual nucleus has a uniform and well-rounded shape. It is interesting to note that these tumor cells are also surrounded by collagen fibers as shown in Figure 3F, and this suggests that tumor invasion has caused a desmoplastic response. It is apparent that SHG imaging is prominent to look into collagen fiber network distributing in the extracellular matrices, which cannot be obtained directly

from conventional optical microscopy of H&E-stained sections. As a consequence, TPAF imaging combined with SHG imaging is very helpful in understanding the spatial distribution of various tissue components, and may also contribute to our understanding of their interactions.

As we all know, depth of tumor invasion is one of the significant predictors of survival, and treatment is usually

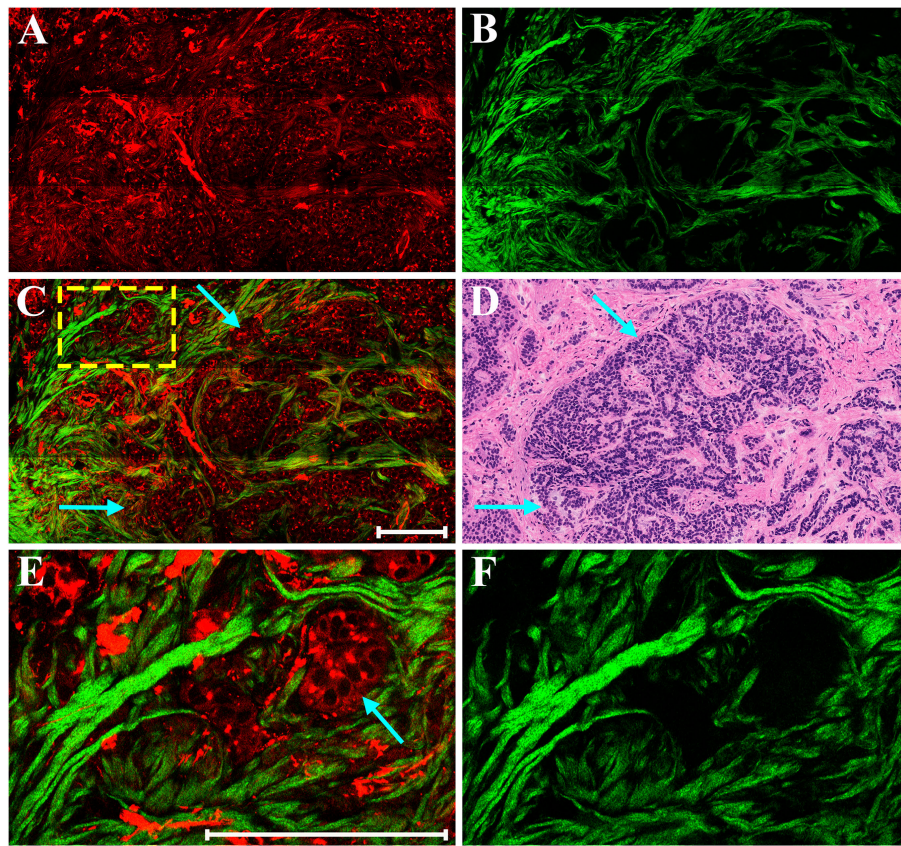


FIGURE 4. MPM images of neuroendocrine tumors invading into submucosa and a corresponding H&E-stained image: (A) TPAF image; (B) SHG image; (C) Composite image; (D) H&E-stained image ($40\times$); and (E-F) Magnified MPM and SHG images of the region of interest (yellow dashed square) respectively. Pseudo-color presentation in the MPM image: red—TPAF; green—SHG. Cyan arrow: neuroendocrine tumor cells. Scale bar: $100\mu\text{m}$.

based on the invasion depth. Therefore, for the early gastrointestinal neuroendocrine neoplasms, we further studied the histopathological changes in the submucosal layer caused by tumor invasion according to multiphoton imaging. As displayed in Figure 4, MPM clearly demonstrates the pathologic features of the submucosa following tumor invasion. Normal submucosa is mainly composed of a great many of collagen fibers, blood vessels, lymphatics and so on; however, multiphoton imaging reveals that the normal submucosal structure is seriously damaged with the invasion of neuroendocrine tumors: firstly, a large number of tumor cells (cyan arrow in Figure 4C) can be seen through TPAF signal; secondly, many collagen fibers have been degraded and the remaining fibers become disorganized and fragmented by SHG signal. The region of interest (yellow dashed square in Figure 4C) is magnified in Figure 4E, more clearly showing the spatial distribution between tumor cells (cyan arrow in Figure 4E) and collagen fibers. These results suggest that MPM is capable of imaging tissue microstructure at a cellular level.

B. AUTOMATED IMAGE ANALYSIS ON SHG IMAGES

In order to quantify the difference between normal and abnormal tissues, we performed automatic image analysis

on SHG images and two quantitative characteristics were achieved. To be specific, we quantified collagen changes in the mucosa and submucosa by the SHG average intensity and collagen density as shown in Figure 5. On one hand, in our research we do not find significant difference in the SHG average intensity between the normal and abnormal mucosa (54.05 ± 8.47 versus 48.37 ± 20.77), but the SHG average intensity in abnormal submucosa (78.80 ± 16.55) is visibly decreased by comparing with that in the healthy submucosa (117.81 ± 6.51), and it must be said that the standard deviations of the average intensity are especially large in the abnormal mucosa and submucosa, reflecting the large difference in tumor microenvironment between different patients. On the other hand, quantitative data reveal that collagen density in the abnormal mucosa (0.11 ± 0.03) is larger than that in normal mucosa (0.08 ± 0.02), directly verifying the desmoplastic reaction induced by tumor invasion, and quantitative results also uncover that collagen density in the healthy submucosa is 0.36 ± 0.08 , while in abnormal submucosa it decreases to 0.17 ± 0.05 , ulteriorly confirming that collagen degradation happens with neuroendocrine tumors invading into submucosa. These results suggest that MPM is capable of qualitatively as well as quantitatively monitoring the changes in mucosa and submucosa during

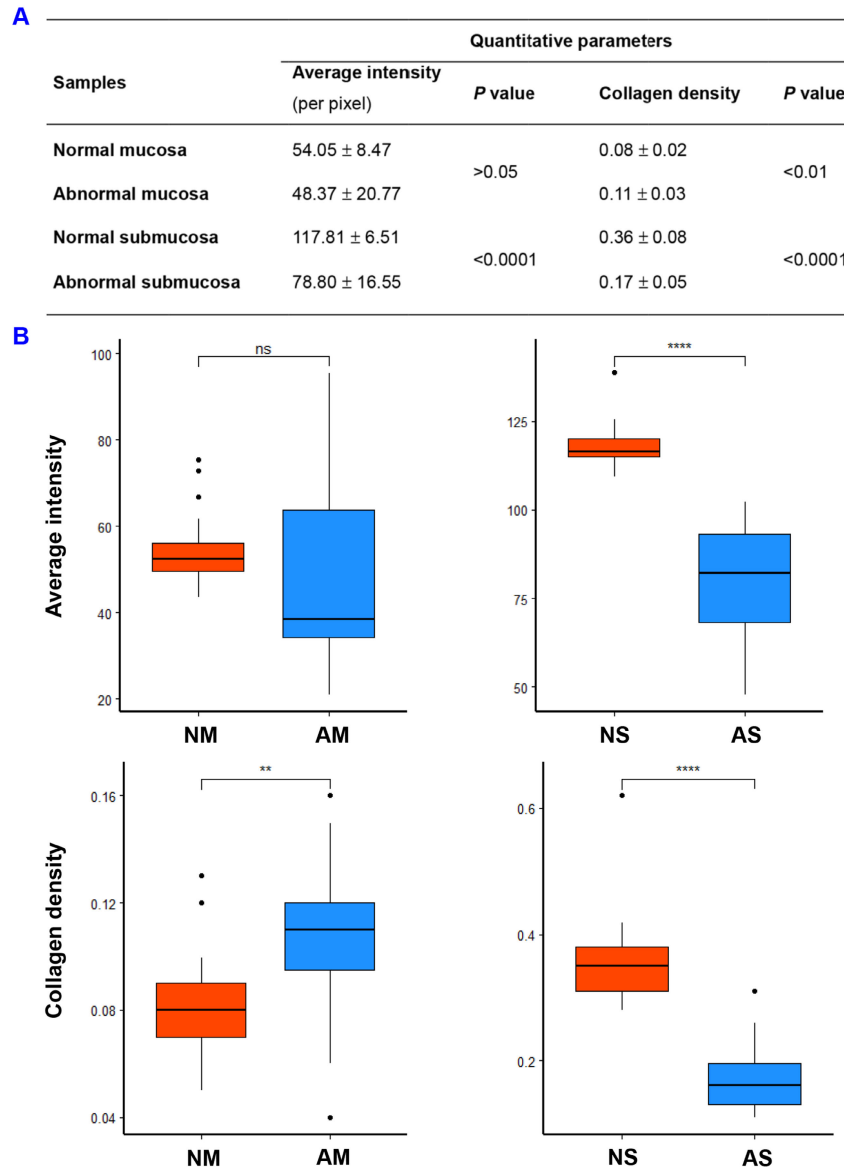


FIGURE 5. (A) Two quantified collagen features for differentiating the normal from abnormal tissues; (B) A box-plot showing the data distribution from normal and cancerous tissues. NM: normal mucosa; AM: abnormal mucosa; NS: normal submucosa; AS: abnormal submucosa. ** denotes $P < 0.01$, **** denotes $P < 0.0001$, and ns denotes no significant difference.

mammary carcinogenesis without a need for exogenous contrast agent.

IV. DISCUSSION

Although neuroendocrine tumors are rare neoplasms, they have a malignant potential, and most of them occur in the gastrointestinal tract [23], [24]. Even today, these tumors remain a clinical challenge because of their heterogeneity in biological behavior, diagnosis as well as treatment options. Gastric neuroendocrine tumors are rarely malignant, but the incidence has been rising recently maybe due to advances in diagnostic technology or increasing public awareness about these diseases [25]. There is still a possibility of recurrence

and metastasis of gastrointestinal neuroendocrine tumors, although their prognosis is often better by comparing with other gastrointestinal cancers [26], [27]. For all neuroendocrine tumors, the prognosis has much improved with the decline in the diagnosis of advanced tumors [28], [29], suggesting that early diagnosis plays an important role in improving prognosis and survival rate. However, many patients are still diagnosed with advanced disease [30], [31], because these tumors are often asymptomatic at an early stage. Endoscopic screening is the only reliable way to find these tumors at present, but its accuracy remains to be improved in identifying small tumors and assessing the depth of tumor invasion [32].

For early gastrointestinal neuroendocrine neoplasms, main research should focus on the detection of small tumors and the histopathological changes in the mucosa and submucosa caused by tumor invasion. Tumor size was reported to be one of the most relevant factors affecting patient management [33], [34]. However, small neuroendocrine tumors are hard to spot since they rarely cause specific symptoms. In most instances, these tumors are discovered by accident during an endoscopic examination which is performed for another purpose. An important factor in the detection of single cell or small tumor nest is the exploitation of a new kind of optical diagnostic technique which has the ability to visualize biological organization at subcellular resolution. Fortunately, a novel optical imaging technique—MPM has been developed. The development of MPM has circumvented many limitations such as poor penetration depth, photo-bleaching and photo-damage of biological tissues during imaging. This microscope has also made significant advances in the biological visualization of cellular and subcellular events, and consequently is regarded as a potentially reliable tool for presurgical assessment of various diseases [35], [36].

In this work, TPAF image can potentially provide the morphological and structural information in a similar way to standard histology and therefore can offer an approach to identify small neuroendocrine tumors, small tumor nests and even single tumor cell, while SHG image can accurately monitor changes in the extracellular matrix such as desmoplasia induced by tumor invasion and as a result is helpful to accurately locate the spatial distribution of tumor cells. Moreover, accurate diagnosis of the depth of tumor infiltration plays a critical role in formulating follow-up treatment strategies and evaluating prognosis of patients. Endoscopic resection followed by periodic endoscopic monitoring is the preferred treatment towards the early neuroendocrine tumors of gastrointestinal tract [37]. Several conventional examination techniques including Computed Tomography (CT), Magnetic Resonance Imaging (MRI), Endoscopic Ultrasonography (EUS), Positron Emission Tomography (PET)/CT, and so on, have been used for evaluating tumor invasion depth [38], [39], but these techniques can only provide rough diagnostic information and are difficult to accurately diagnose tumor performance due to technical limitations such as low resolution, et al [40]. Our imaging results reveal that MPM can well identify the histopathological features of tumors at different invasion depths and therefore may help determine the depth of tumor infiltration.

Furthermore, we used automatic image analysis to analyze the SHG images and extracted two optical diagnostic parameters, namely the SHG average intensity and collagen density, to quantify the changes in tumor microenvironment. The analysis results manifest that there is no difference in the average intensity between normal and abnormal mucosa ($P>0.05$), but has a significant difference between the two groups in the collagen content ($P<0.01$). Quantitative analysis also reveals obvious differences in the average intensity and collagen content between normal and abnormal submucosa

($P<0.0001$). It must be pointed out that more samples are needed to verify the validity of these two optical characteristic parameters.

In summary, early gastrointestinal neuroendocrine tumors which are generally defined as the tumor confined to the mucosa or submucosa have the characteristics of low risk and a better cancer-related survival. Early detection and treatment of these precancerous or malignant lesions remains the most important to reduce mortality. This study highlights the unique advantage of multiphoton imaging in identifying early gastrointestinal neuroendocrine neoplasms at a subcellular resolution without the need for exogenous fluorescent dyes. In view of the limitations of current clinical examination techniques, it is necessary to develop a real-time, unlabeled technique with comparable histological diagnosis during routine endoscopy, and thus many researchers have been working on multiphoton endoscope [41]–[44]. It was reported that a miniaturized multiphoton probe has been developed and could serve as a flexible test bench for exploring a clinical multiphoton endoscope [45]. Moreover, MPM is capable of deep tissue imaging up to ~ 1000 microns at present [46], [47], and has the ability to perform three-dimensional imaging (optical section imaging) [48], [49]. Hence there is reason to believe that MPM, once it can be clinical use as a screening tool in the near future, will greatly improve the early diagnosis of gastrointestinal neuroendocrine tumors.

ACKNOWLEDGMENT

(Lianhuang Li, Shenghui Huang, Lida Qiu, and Weizhong Jiang contributed equally to this work.)

REFERENCES

- [1] X. Zhu, H. Jing, and T. Yao, “Clinical characteristics of early neuroendocrine carcinoma in stomach: A case report and review of literature,” *Medicine*, vol. 98, no. 30, Jul. 2019, Art. no. e16638.
- [2] L. Ellis, M. J. Shale, and M. P. Coleman, “Carcinoid tumors of the gastrointestinal tract: Trends in incidence in england since 1971,” *Amer. J. Gastroenterol.*, vol. 105, no. 12, pp. 2563–2569, Dec. 2010.
- [3] H. Scherubl, “Options for gastroenteropancreatic neuroendocrine tumours,” *Lancet Oncol.*, vol. 9, no. 3, p. 203, Mar. 2008.
- [4] C. R. Gluckman and D. C. Metz, “Gastric neuroendocrine tumors (Carcinoids),” *Current Gastroenterol. Rep.*, vol. 21, no. 4, p. 13, Apr. 2019.
- [5] J. B. Marshall and G. Bodnarchuk, “Carcinoid tumors of the gut: Our experience over three decades and review of the literature,” *J. Clin. Gastroenterol.*, vol. 16, no. 2, pp. 123–129, Mar. 1993.
- [6] I. M. Modlin, I. Latch, M. Zikusoka, M. Kidd, G. Eick, and A. K. C. Chan, “Gastrointestinal carcinoids: The evolution of diagnostic strategies,” *J. Clin. Gastroenterol.*, vol. 40, no. 7, pp. 572–582, Aug. 2006.
- [7] H. Scherubl, R. T. Jensen, G. Cadot, U. Stölzel, and G. Klöppel, “Management of early gastrointestinal neuroendocrine neoplasms,” *World J. Gastrointest Endosc.*, vol. 3, no. 7, pp. 133–139, 2011.
- [8] S. Zhang, Y. X. Tong, X. H. Zhang, Y. J. Zhang, X. S. Xu, A. T. Xiao, and T. F. Chao, “A novel and validated nomogram to predict overall survival for gastric neuroendocrine neoplasms,” *J. Cancer*, vol. 10, no. 24, pp. 5944–5954, 2019.
- [9] O. Rorstad, “Prognostic indicators for carcinoid neuroendocrine tumors of the gastrointestinal tract,” *J. Surgical Oncol.*, vol. 89, no. 3, pp. 151–160, 2005.
- [10] J. Strosberg, N. Gardner, and L. Kvols, “Survival and prognostic factor analysis of 146 metastatic neuroendocrine tumors of the mid-gut,” *Neuroendocrinology*, vol. 89, no. 4, pp. 471–476, 2009.

- [11] I. M. Modlin, K. D. Lye, and M. Kidd, "A 5-decade analysis of 13,715 carcinoid tumors," *Cancer*, vol. 97, no. 4, pp. 934–959, Feb. 2003.
- [12] M. Jain, N. Narula, A. Aggarwal, B. Stiles, M. M. Shevchuk, J. Sterling, B. Salamoon, V. Chandel, W. W. Webb, N. K. Altorki, and S. Mukherjee, "Multiphoton microscopy: A potential 'optical biopsy' tool for real-time evaluation of lung tumors without the need for exogenous contrast agents," *Arch. Pathol. Lab. Med.*, vol. 138, no. 8, pp. 1037–1047, 2014.
- [13] L. Li, D. Kang, C. Feng, S. Zhuo, H. Tu, Y. Zhou, and J. Chen, "Label-free assessment of premalignant gastric lesions using multimodal nonlinear optical microscopy," *IEEE J. Sel. Topics Quantum Electron.*, vol. 25, no. 1, Jan./Feb. 2019, Art. no. 7200806.
- [14] H. H. Tu, Y. Liu, D. Turchinovich, M. Marjanovic, J. K. Lyngsø, J. Lægsgaard, E. J. Chaney, Y. Zhao, S. You, W. L. Wilson, and B. Xu, "Stain-free histopathology by programmable supercontinuum pulses," *Nature Photon.*, vol. 10, no. 8, pp. 534–541, 2016.
- [15] H. Mehidine, M. Sibai, F. Poulon, J. Pallud, P. Varlet, M. Zanello, B. Devaux, and D. A. Haidar, "Multimodal imaging to explore endogenous fluorescence of fresh and fixed human healthy and tumor brain tissues," *J. Biophotonics*, vol. 12, no. 3, Mar. 2019, Art. no. e201800178.
- [16] X. Li, H. Li, X. He, T. Chen, X. Xia, C. Yang, and W. Zheng, "Spectrum- and time-resolved multiphoton signals reveal quantitative differentiation of premalignant and malignant gastric mucosa," *Biomed Opt Express*, vol. 9, no. 2, pp. 453–471, 2018.
- [17] T.-L. Sun, Y. Liu, M.-C. Sung, H.-C. Chen, C.-H. Yang, V. Hovhannissyan, W.-C. Lin, Y.-M. Jeng, W.-L. Chen, L.-L. Chiou, G.-T. Huang, K.-H. Kim, P. T. C. So, Y.-F. Chen, H.-S. Lee, and C.-Y. Dong, "Ex vivo imaging and quantification of liver fibrosis using second-harmonic generation microscopy," *J. Biomed. Opt.*, vol. 15, no. 3, 2010, Art. no. 036002.
- [18] L. Li, D. Kang, Z. Huang, Z. Zhan, C. Feng, Y. Zhou, H. Tu, S. Zhuo, and J. Chen, "Multimodal multiphoton imaging for label-free monitoring of early gastric cancer," *BMC Cancer*, vol. 19, no. 1, p. 295, Dec. 2019.
- [19] N. Otsu, "A threshold selection method from gray-level histograms," *IEEE Trans. Syst., Man., Cybern.*, vol. SMC-9, no. 1, pp. 62–66, Jan. 1979.
- [20] I. M. Modlin and A. Sandor, "An analysis of 8305 cases of carcinoid tumors," *Cancer*, vol. 79, no. 4, pp. 813–829, Sep. 2000.
- [21] S. Hoteya, T. Iizuka, D. Kikuchi, and N. Yahagi, "Endoscopic submucosal dissection for gastric submucosal tumor, endoscopic sub-tumoral dissection," *Digestive Endoscopy*, vol. 21, no. 4, pp. 266–269, Oct. 2009.
- [22] S. Suzuki, N. Ishii, M. Uemura, G. A. Deshpande, M. Matsuda, Y. Iizuka, K. Fukuda, K. Suzuki, and Y. Fujita, "Endoscopic submucosal dissection (ESD) for gastrointestinal carcinoid tumors," *Surgical Endoscopy*, vol. 26, no. 3, pp. 759–763, 2012.
- [23] H. Y. Park, M. J. Kwon, H. S. Kang, Y. J. Kim, N. Y. Kim, M. J. Kim, K.-W. Min, K. C. Choi, E. S. Nam, S. J. Cho, H.-R. Park, S. K. Min, J. Seo, J.-Y. Choe, and H. K. Lee, "Targeted next-generation sequencing of well-differentiated rectal, gastric, and appendiceal neuroendocrine tumors to identify potential targets," *Hum. Pathol.*, vol. 87, pp. 83–94, May 2019.
- [24] R. Garcia-Carbonero, J. Capdevila, G. Crespo-Herrero, J. A. Díaz-Pérez, M. P. M. del Prado, V. A. Orduña, I. Sevilla-García, C. Villabona-Artero, A. Beguiristain-Gómez, M. Llanos-Muñoz, M. Marazuela, C. Alvarez-Escola, D. Castellano, E. Vilar, P. Jiménez-Fonseca, A. Teulé, J. Sastre-Valera, M. Benavent-Viñuelas, A. Monleon, and R. Salazar, "Incidence, patterns of care and prognostic factors for outcome of gastroenteropancreatic neuroendocrine tumors (GEP-NETs): Results from the national cancer registry of spain (RGETNE)," *Ann. Oncol.*, vol. 21, no. 9, pp. 1794–1803, Sep. 2010.
- [25] A. Dasari, C. Shen, D. Halperin, B. Zhao, S. Zhou, Y. Xu, T. Shih, and J. C. Yao, "Trends in the incidence, prevalence, and survival outcomes in patients with neuroendocrine tumors in the United States," *JAMA Oncol.*, vol. 3, no. 10, pp. 1335–1342, 2017.
- [26] C. Fang, W. Wang, Y. Zhang, X. Feng, J. Sun, Y. Zeng, Y. Chen, Y. Li, M. Chen, Z. Zhou, and J. Chen, "Clinicopathologic characteristics and prognosis of gastroenteropancreatic neuroendocrine neoplasms: A multicenter study in south China," *Chin. J. Cancer*, vol. 36, no. 1, p. 51, Dec. 2017.
- [27] K. K. Turaga and L. K. Kvols, "Recent progress in the understanding, diagnosis, and treatment of gastroenteropancreatic neuroendocrine tumors," *CA A, Cancer J. Clinicians*, vol. 61, no. 2, pp. 113–132, Mar. 2011.
- [28] I. M. Modlin, K. Oberg, D. C. Chung, R. T. Jensen, W. W. de Herder, R. V. Thakker, M. Caplin, G. D. Fave, G. A. Kaltsas, E. P. Krenning, and S. F. Moss, "Gastroenteropancreatic neuroendocrine tumours," *Lancet Oncol.*, vol. 9, no. 1, pp. 61–72, 2008.
- [29] C. S. Landry, G. Brock, C. R. Scoggins, K. M. McMasters, and R. C. G. Martin, "A proposed staging system for gastric carcinoid tumors based on an analysis of 1,543 patients," *Ann. Surgical Oncol.*, vol. 16, no. 1, pp. 51–60, Jan. 2009.
- [30] J. A. Söreide, J. A. van Heerden, G. B. Thompson, C. Schleck, D. M. Ilstrup, and M. Churchward, "Gastrointestinal carcinoid tumors: Long-term prognosis for surgically treated patients," *World J. Surg.*, vol. 24, no. 11, pp. 1431–1436, Nov. 2000.
- [31] K. O. Shebani, W. W. Souba, D. M. Finkelstein, P. C. Stark, K. M. Elgadi, K. K. Tanabe, and M. J. Ott, "Prognosis and survival in patients with gastrointestinal tract carcinoid tumors," *Ann. Surg.*, vol. 229, no. 6, pp. 815–821, 1999.
- [32] S. Mocellin and S. Pasquali, "Diagnostic accuracy of endoscopic ultrasound (EUS) for the preoperative locoregional staging of primary gastric cancer," *Cochrane Database Systematic Rev.*, vol. 2, Feb. 2015, Art. no. CD009944.
- [33] F. Panzuto, D. Campana, S. Massironi, A. Faggiano, M. Rinzivillo, G. Lamberti, V. Sciola, E. Lahner, L. Manuzzi, A. Colao, and B. Annibale, "Tumour type and size are prognostic factors in gastric neuroendocrine neoplasia: A multicentre retrospective study," *Digestive Liver Disease*, vol. 51, no. 10, pp. 1456–1460, Oct. 2019.
- [34] K. D. Gray, M. D. Moore, S. Panjwani, A. Elmously, C. Afaneh, T. J. Fahey, and R. Zarnegar, "Predicting survival and response to treatment in gastroesophageal neuroendocrine tumors: An analysis of the national cancer database," *Ann. Surgical Oncol.*, vol. 25, no. 5, pp. 1418–1424, May 2018.
- [35] E. E. Hoover and J. A. Squier, "Advances in multiphoton microscopy technology," *Nature Photon.*, vol. 7, no. 2, pp. 93–101, Feb. 2013.
- [36] G. Thomas, J. van Voskuilen, H. C. Gerritsen, and H. J. C. M. Sterenborg, "Advances and challenges in label-free nonlinear optical imaging using two-photon excitation fluorescence and second harmonic generation for cancer research," *J. Photochemistry Photobiol. B, Biol.*, vol. 141, pp. 128–138, Dec. 2014.
- [37] M. Tsoli, E. Chatzellis, A. Koumarianou, D. Kolomodi, and G. Kaltsas, "Current best practice in the management of neuroendocrine tumors," *Therapeutic Adv. Endocrinol. Metabolism*, vol. 10, Jan. 2019, Art. no. 2042018818804698.
- [38] K. He, L. Zhao, X. Huang, Y. Ding, L. Liu, X. Wang, M. Wang, Y. Zhang, and Z. Fan, "Label-free imaging for t staging of gastric carcinoma by multiphoton microscopy," *Lasers Med. Sci.*, vol. 33, no. 4, pp. 871–882, May 2018.
- [39] C. Han, R. Lin, H. Shi, J. Liu, W. Qian, Z. Ding, and X. Hou, "The role of endoscopic ultrasound on the preoperative t staging of gastric cancer: A retrospective study," *Medicine*, vol. 95, no. 36, p. e4580, Sep. 2016.
- [40] R. Weissleder and M. J. Pittet, "Imaging in the era of molecular oncology," *Nature*, vol. 452, no. 7187, pp. 580–589, Apr. 2008.
- [41] D. R. Rivera, C. M. Brown, D. G. Ouzounov, W. W. Webb, and C. Xu, "Multifocal multiphoton endoscope," *Opt. Lett.*, vol. 37, no. 8, pp. 1349–1351, Apr. 2012.
- [42] C. Wang and N. Ji, "Characterization and improvement of three-dimensional imaging performance of GRIN-lens-based two-photon fluorescence endomicroscopes with adaptive optics," *Opt. Express*, vol. 21, no. 22, pp. 27142–27154, 2013.
- [43] C. Lefort, H. Hamzeh, F. Louradour, F. Pain, and D. A. Haidar, "Characterization, comparison, and choice of a commercial double-clad fiber for nonlinear endomicroscopy," *J. Biomed. Opt.*, vol. 19, no. 7, Jul. 2014, Art. no. 076005.
- [44] R. Le Harzic, M. Weinigel, I. Riemann, K. König, and B. Messerschmidt, "Nonlinear optical endoscope based on a compact two axes piezo scanner and a miniature objective lens," *Opt. Express*, vol. 16, no. 25, pp. 20588–20596, 2008.
- [45] C. L. Hoy, N. J. Durr, P. Chen, W. Piyawattanametha, H. Ra, O. Solgaard, and A. Ben-Yakar, "Miniaturized probe for femtosecond laser microsurgery and two-photon imaging," *Opt. Express*, vol. 16, no. 13, pp. 9996–10005, 2008.
- [46] V. Crosignani, A. S. Dvornikov, J. S. Aguilar, C. Stringari, R. A. Edwards, W. W. Mantulin, and E. Gratton, "Deep tissue fluorescence imaging and *in vivo* biological applications," *J. Biomed. Opt.*, vol. 17, no. 11, 2012, Art. no. 116023.
- [47] D. R. Miller, J. W. Jarrett, A. M. Hassan, and A. K. Dunn, "Deep tissue imaging with multiphoton fluorescence microscopy," *Current Opinion Biomed. Eng.*, vol. 4, no. 12, pp. 32–39, Dec. 2017.

- [48] B. Wen, K. R. Campbell, K. Tilbury, O. Nadiarnykh, M. A. Brewer, M. Patankar, V. Singh, K. W. Eliceiri, and P. J. Campagnola, “3D texture analysis for classification of second harmonic generation images of human ovarian cancer,” *Sci. Rep.*, vol. 6, no. 1, p. 35734, Dec. 2016.
- [49] Y. Sun, S. You, H. Tu, D. R. Spillman, E. J. Chaney, M. Marjanovic, J. Li, R. Barkalifa, J. Wang, A. M. Higham, N. N. Luckey, K. A. Cradock, Z. G. Liu, and S. A. Boppart, “Intraoperative visualization of the tumor microenvironment and quantification of extracellular vesicles by label-free nonlinear imaging,” *Sci. Adv.*, vol. 4, no. 12, Dec. 2018, Art. no. eaau5603.



ZHIFEN CHEN is currently a Colorectal Surgeon with the Fujian Medical University Union Hospital, China. His research interest includes application of nonlinear optical microscopy in colorectal cancer.



DEYONG KANG is currently an Associate Chief Physician with the Fujian Medical University Union Hospital, China. His research interest includes clinicopathology of gastrointestinal tumors.



LIANHUANG LI is currently an Associate Researcher with Fujian Normal University, China. His main research interests include multiphoton imaging and biomedical photonics.



SHENGHUI HUANG is currently a Colorectal Surgeon and an Associate Chief Physician with the Fujian Medical University Union Hospital, China. His research interests include basic and clinical researches of colorectal surgery and application of nonlinear spectral imaging in colorectal cancer.



LIDA QIU is currently pursuing the Ph.D. degree with Fujian Normal University. He is an Associate Professor with Minjiang University, China. His research interests include image processing and artificial intelligence.



JIANXIN CHEN was born in Heilongjiang, China, in 1970. She is currently the Director of the Key Laboratory of Optoelectronic Science and Technology for Medicine of Ministry of Education. Her research interests include development and applications of nonlinear optical microscopy in biological and biomedical research.



WEIZHONG JIANG received the Ph.D. degree in general surgery from Fujian Medical University, Fuzhou, China, in 2011. He is currently a Colorectal Surgeon and an Associate Chief Physician with the Fujian Medical University Union Hospital. His research interest includes basic and clinical researches of colorectal surgery.



YONGJIAN ZHOU received the M.D. degree in general surgery from Peking University, China, in 2005. He is currently a Chief Physician and a Professor of surgery with the Fujian Medical University Union Hospital, China. His research interests include basic and clinical researches of digestive surgery and applications of nonlinear optical microscopy in colorectal and gastric cancer.